Acceleration in thinning rate on western Svalbard glaciers

J. Kohler,[1] T. D. James,[2] T. Murray,[2] C. Nuth,[1] O. Brandt,[1] N. E. Barrand,[2] H. F. Aas,[1] and A. Luckman[2]

Received 25 May 2007; revised 30 June 2007; accepted 2 August 2007; published 21 September 2007.

[1] Geodetic measurements indicate that a number of glaciers in western Svalbard ranging in size from 5–1000 km^2 are losing mass at an accelerating rate. The average thinning rate for Midtre Lovénbreen, the glacier with the best data coverage, has increased steadily since 1936. Thinning rates for 2003–2005 are more than 4 times the average for the first measurement period 1936–1962 and are significantly greater than presented previously. On Slakbreen, thinning rates for the latest measurement period 1990–2003 are more than 4 times that of the period 1961–1977. Thinning of several glaciers along a previously measured airborne lidar profile in Wedel Jarls Land has also increased, doubling between the period 1990–1996 and 1996–2002. Our results imply an increased sea level contribution from Svalbard. In addition, the mass loss is an important influence on measured rates of rebound on western Svalbard and should be factored into analysis of GRACE results. **Citation:** Kohler, J., T. D. James, T. Murray, C. Nuth, O. Brandt, N. E. Barrand, H. F. Aas, and A. Luckman (2007), Acceleration in thinning rate on western Svalbard glaciers, *Geophys. Res. Lett.*, *34*, L18502, doi:10.1029/2007GL030681.

1. Introduction

[2] Global climate models predict that the Arctic will experience greater than global average temperature and precipitation increases in response to build-up of greenhouse gases [e.g., *ACIA*, 2005]. Recent observations indicate that important climate-induced changes are indeed underway in the High Arctic, including: warming of the troposphere [*Santer et al.*, 2005]; reduction [*Stroeve et al.*, 2005] and thinning [*Lindsay and Zhang*, 2005] of sea ice cover; decrease in snow cover area [*Comiso*, 2006]; warming of tundra permafrost [*Serreze et al.*, 2000]; and changes in the geometry and dynamics of the Greenland ice sheet [*Luckman et al.*, 2006, *Rignot and Kanagaratnam*, 2006, *Thomas et al.*, 2006]. Small glaciers (i.e., ice masses outside of the Greenland and Antarctic ice sheets) are losing mass overall, and have been predicted to contribute a significant amount to sea-level rise up to 2100, second only to ocean volume change due to thermal expansion [*Church et al.*, 2001; *Kaser et al.*, 2006].

[3] Svalbard is one of the larger repositories of Arctic land ice outside of the Greenland ice sheet. Nearly 60% of Svalbard is glaciated (3.6×10^4 km^2), representing ~10% of the total Arctic small glacier area. The archipelago lies at the northern extremity of the warm North Atlantic current and is sensitive to climate shifts [*Hagen et al.*, 2003a]. Svalbard has been estimated to contribute as much as 0.06 mm a^{-1} to sea level rise [*Dowdeswell et al.*, 1997; *Van de Wal and Wild*, 2001], although other estimates have been more modest (0.01–0.04 mm a^{-1}) [*Hagen et al.*, 2003a, 2003b].

[4] Since the early part of the 20th century Svalbard glacier fronts have been thinning and retreating, while ice thickness has been increasing at the uppermost elevations in many locations [*Bamber et al.*, 2004; *Nuth et al.*, 2007], the same pattern observed in Greenland and the Canadian Arctic [*Abdalati et al.*, 2004; *Thomas et al.*, 2006]. Here we use geodetic methods to show that the rate of volume loss from two Svalbard glaciers (Figure 1), Midtre Lovénbreen (ML) and Slakbreen (SL), has been increasing, with significantly higher thinning rates during the most recent measurement periods. Furthermore, we analyze surface elevation profiles collected with airborne lidar over several glaciers in Wedel Jarls Land (WJ), in southern Svalbard (Figure 1), to show the same trend applies to a larger area of Svalbard.

[5] ML (Figure 1a) located in NW Svalbard near Ny-Ålesund, is a small valley glacier oriented in a N-NE direction, with a surface area of 5.2 km^2, a length of 3.2 km along its centerline, and elevations ranging from 50–650 m asl. SL (Figure 1b), located on the north side of Van Mijenfjorden near Sveagruva, is a larger E-W oriented valley glacier, with a surface area of 41.5 km^2, a length of 13.5 km, and an elevation range of 170–900 m asl. Neither glacier is thought to be surge-type [*Jiskoot et al.*, 2000].

[6] Surface elevation profiles in WJ extend from Bellsund to Hornsund to cover several glaciers in the Amundsisen ice cap (details are given by *Bamber et al.* [2005]), and are representative for a large area (ca. 1000 km^2) of southern Svalbard, extending from sea level up to ~800 m asl. Only one of the profiled glaciers in WJ is known to be surge-type (Recherchebreen), having last surged in 1948 [*Hagen et al.*, 1993].

2. Data and Methods

[7] The data consist of contour maps, digital elevation models (DEMs) made from either airborne lidar swath data or conventional photogrammetry, and airborne lidar profiles (Table 1). Map contours were digitized and converted to a common datum and projection (WGS84, UTM zone 33 north) using a 7-parameter transformation. Lidar data were collected on ML and SL in 2003 and 2005 using an Optech ALTM3033 instrument. Comparison of these lidar spot heights with independently surveyed differential GPS data shows that elevation accuracy is within ±0.25 m. Lidar data were interpolated to 5 m regularly-spaced grids using

[1] Norwegian Polar Institute, Polar Environmental Centre, Tromsø, Norway.
[2] School of the Environment and Society, Swansea University, Swansea, UK.

0094-8276/07/2007GL030681$05.00

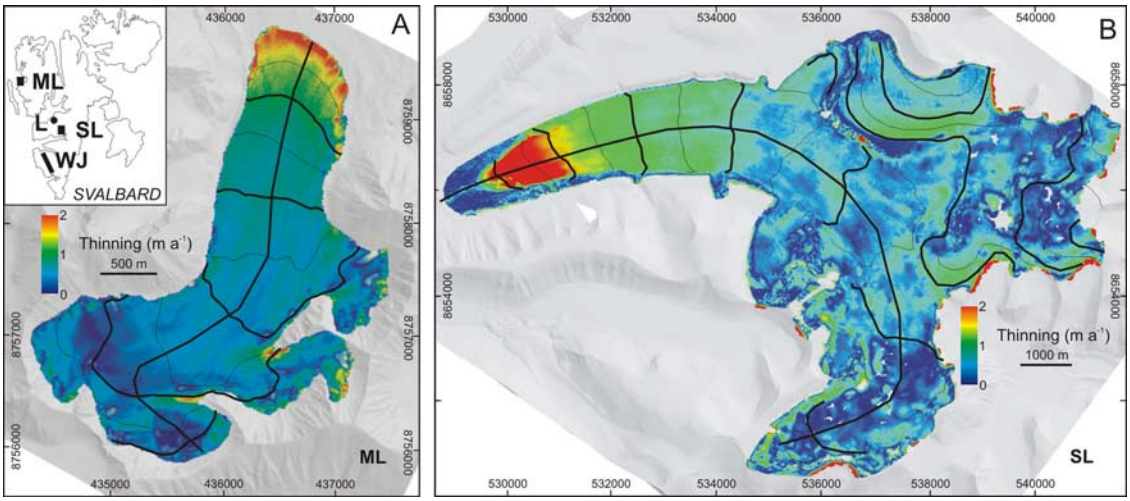

Figure 1. Difference DEMs showing rate of elevation change for (a) ML, 2003–2005, and (b) SL, 1990–2003. Contours are spaced at 50 m intervals, bold contours at 100 m intervals, and the lowest bold contour on each glacier is at 200 m relative to the ellipsoid. Grids are UTM in meters. Background is shaded relief lidar DEM. Insert shows Svalbard with location of glaciers and meteorological station at Longyearbyen (L), heavy line (WJ) is location of ATM lidar profile.

an adapted Delauney triangulation gridding algorithm. Photogrammetric DEMs were created using archived aerial photography, with ground control either from conventional ground survey points or from the lidar-derived DEMs (Table 1) [*James et al.*, 2006]. Ice-surface elevation profiles over WJ were acquired with NASA's Airborne Topographic Mapper (ATM) in the springs of 1996 and 2002 [*Bamber et al.*, 2005]. The technical details of the ATM are described elsewhere [*Krabill et al.*, 2000]; vertical accuracies are estimated to be 0.1 m or better [*Bamber et al.*, 2005].

[8] For ML and SL the 2003 lidar DEM was used as the reference. Elevation changes for the DEMs were obtained by subtraction. Changes in elevation between the contour maps and reference DEM were calculated by interpolating into the reference DEM at the locations of the digitized contour points. These differences, located along the original contours, are then interpolated to make an elevation difference DEM on the same regular 5 m grid as the reference DEM. We also interpolate elevation changes along the centerline profiles of ML and SL, which are sampled at 10 m intervals, and average the differences into 50 m elevation bins to smooth the data.

[9] Elevation changes for ML and SL were averaged over the entire surface using pixel summation [e.g., *Etzelmüller et al.*, 1993] of the difference fields between two epochs. Total volume change ΔV was obtained by summing the i difference values ($h_{i1} - h_{i2}$) for each pair of epochs 1 and 2 contained within the larger glacier surface area A (epoch 1 in all cases) and multiplying by the area l_p^2 represented by each grid point, where l_p is the grid spacing: $\Delta V = l_p^2 \sum_A (h_{i1} - h_{i2})$. The mean elevation change is then given by $\overline{dh/dt} = \Delta V/(\overline{A}\Delta t)$, where $\overline{A}$ is the area averaged over the two epochs, and Δt is the length of time between epochs [*Arendt et al.*, 2002].

[10] The vertical datums of the contour maps and photogrammetric DEMs are dependent on a limited number of control points, such that there may be a systematic bias in the mapped elevations. There may also be a bias due to geoid-ellipsoid differences, since the early data are referenced to a mean-sea level datum, while the later data are referenced to a geocentric ellipsoidal datum. If errors were completely independent of each other, the standard error of each $\overline{dH/dt}$ estimate would be reduced by the averaging over the whole glacier. However, there is a degree of spatial autocorrelation in the difference fields, a result of geolocation errors in the original map products. Rather than attempt to characterize this, we simply use one standard deviation of the low-slope non-glaciated land differences, divided by the number of years in the period, as a conservative estimate of $\overline{dH/dt}$ errors.

[11] Biases and errors were estimated from the mean and standard deviation of elevation differences over ice-free land areas whose slopes are less than 20°. Low slope areas were used because small geolocation errors in steep slope areas can lead to apparently large elevation differences. We corrected elevations by removing the mean of the low-slope non-glacier differences, which on ML varied from −0.10 m, between the two lidar epochs, to −1.71 m for the 1969 data. Once the bias has been removed the error of each DEM was assessed using the standard deviation of its difference with the reference DEM for the same low-slope non-glacier data. For the lidar data pair on ML, this standard deviation was 0.36 m, a value comparable to that derived from independently surveyed differential GPS data. Errors are larger at ML for the photogrammetric data and progressively larger still for the older contour maps (Figure 2a). Biases and errors arising from differencing the three most recent SL DEMs were less than for ML DEMs, because of the larger number of control points used in creating the SL DEMs [*James et al.*, 2006].

[12] Points along the 1996 and 2002 ATM lidar profile are differenced into the 1990 reference DEM. The resultant differences are binned by 1990 elevations to estimate mean elevation change as a function of elevation; these are then averaged after weighting using the 1990 hypsometry of the WJ region. The 1936–1990 difference is computed as above for contour maps and DEMs, compensating for the

Table 1. Data Sources for Each Epoch[a]

ML		SL		WJ	
Year	Source	Year	Source	Year	Source
1936	50 m contour map[b]	1936	50 m contour map[b]	1936	50 m contour map[b]
1962	10 m contour map[c]	1961	5 m posting DEM[d]		
1969	10 m contour map[e]				
1977	10 m contour map[e]	1977	5 m posting DEM[d]		
1995	5 m posting DEM[d]	1990	5 m posting DEM[d]	1990	5m posting DEM[d]
2003	Lidar, ground resolution 0.48 m	2003	Lidar, ground resolution 1.7 m	1996	Lidar, ground resolution 3 m
2005	Lidar, ground resolution 0.67 m			2002	Lidar, ground resolution 6 m

[a]Contour maps were converted from European Datum 1950.
[b]From 1:100,000 NPI maps derived from oblique aerial photographs.
[c]From field survey and oblique terrestrial photogrammetry [*Pillewizer*, 1962].
[d]From vertical aerial photographs.
[e]From unpublished NPI maps derived from vertical aerial photographs.

apparent biases between the 1936 contour maps and the 1990 DEM [*Nuth et al.*, 2007]. We do not estimate errors since the lidar points lie almost entirely on glacier ice. Furthermore, the lidar profiles were collected at the end of winter, and thus measure the elevation of the snow surface, unlike all of the other elevation data, which are made over summer surfaces. We compensate for the snow difference for 1990–1996 by subtracting a uniform snow depth of 2 m along the ATM profiles. A single snow depth may not be realistic, but we have no snow measurements along the profiles to improve this estimate. There may also be a small negative bias in the 1996–2002 period since in northwestern Svalbard, at least, there was more snow in 1996 than in 2002 [*Hagen et al.*, 2003b]. If this were the case for WJ as well, then we would calculate a slightly lower thinning rate for the last period.

[13] Finally, we compare the glacier-wide average elevation change on ML to cumulatively summed mass balance data. ML has one of the longest continuous mass balance records (since 1968) in the high Arctic [*Hagen et al.*, 2003b]. The net balance B_n (given in units of m water equivalent) is a single number reflecting the loss or gain averaged for the glacier as a whole, over the course of about one year [*Paterson*, 1994]. Net balance is the sum of the winter balance B_w (measured roughly from Sept.–May) and the summer balance B_s (May–Sept.). The former is obtained from snow-depth soundings, stake height measurements, and snow density measurements, while the latter is obtained directly by comparing stake heights measured in spring and fall. We convert mass to volume change using a mean ice density of 900 kg m^{-3}.

3. Results

[14] The mean rate of elevation change shows a clear increasing trend since the 1960s (Figures 2a and 2b). We calculate mean thinning rates (Figure 2c) from the slope of elevation change for ML and SL. The mean thinning rate for ML, the glacier with the most complete data, is 0.15 m a^{-1} for the first period 1936–1962, although the error bars are also large for this early part of the record. Thinning rates then more than double from 0.20 m a^{-1} for the 1962–1969 period to 0.52 m a^{-1} for the 1995–2003 period. By 2003–2005, the mean thinning rate was equivalent to 0.69 m a^{-1}, representing an increase of over three-fold from the second period and over four-fold from the earliest period (Figure 2c). While the last period is only two years long, there is clearly a significant increase in the thinning rate in

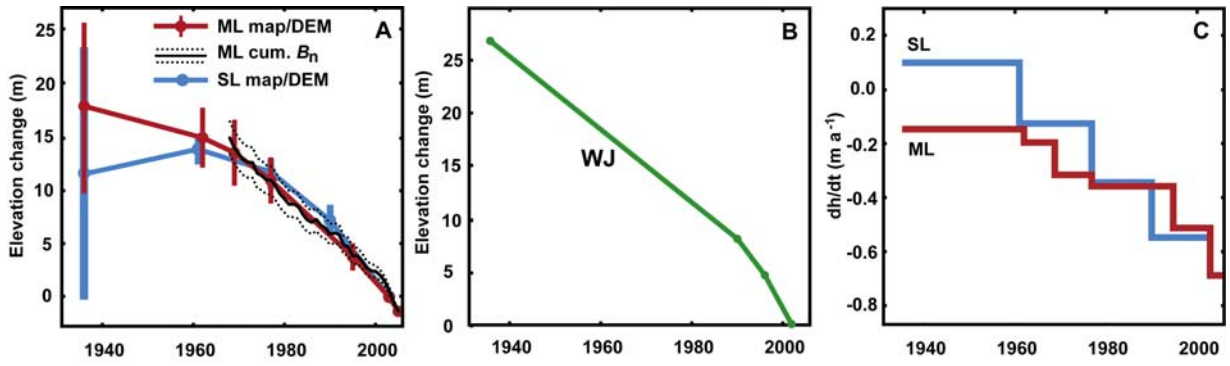

Figure 2. (a) Average elevation change over time for ML and SL, and (b) for WJ, derived from differencing contour maps, DEMs, and lidar profiles. ML and SL are relative to the 2003 DEM, and WJ is relative to 2002. Error bars for ML and SL are one standard deviation of elevation differences in low-slope areas of non-glaciated terrain (see Methods), error is not estimated for WJ. Black line (a) shows cumulatively summed net mass balance on ML from field measurements, converted to units of ice thickness, with accumulated annual error ±25 cm (dashed lines). (c) Average thinning rate on ML and SL for each period obtained from slope of elevation change between epochs.

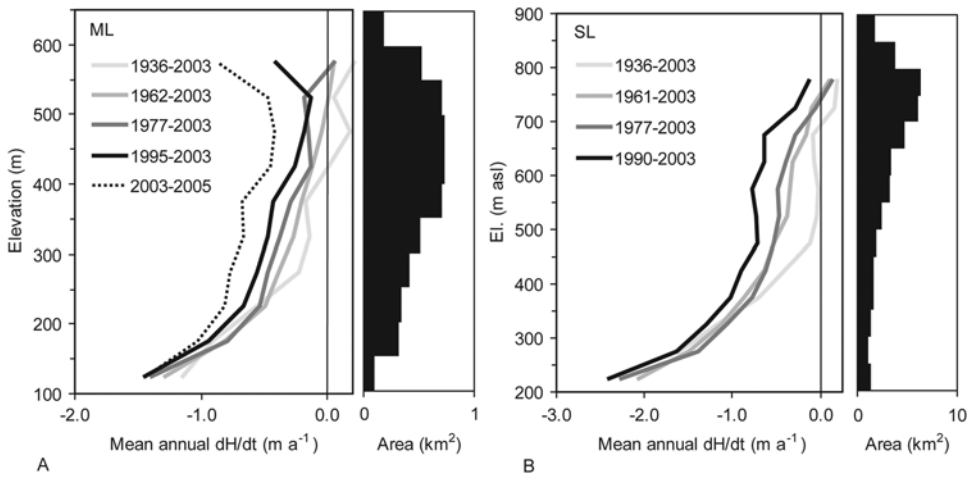

Figure 3. (left) Average annual rate of elevation change along centerline profiles (shown in Figure 1) relative to 2003 and (right) hypsometry in 2003 for (a) ML, and (b) SL. Data are averaged by elevation in 50 m blocks.

each period. This is also shown by the mass balance record (Figure 2a). SL shows an initial thickening for the first period 1936–1961, although the error bars for the 1936 contour map data are very large so this may not be significant (Figure 2a). On SL, thinning rates for the latest measurement period 1990–2003 are more than four times that of the period 1961–1977 (Figure 2c). The increase in thinning is similar for WJ (Figure 2b), with nearly a doubling in the thinning rate comparing the two periods 1990–1996 and 1996–2002.

[15] The recent thinning occurs at all elevation bands of ML and SL (Figure 3), although the greatest changes in rates occur in the upper elevation bands; thinning rates at lower elevations are more uniform. In the early epochs, there is apparent thickening in the upper part of SL (Figure 3). This glacier has a significant portion of its area in the upper elevations, and it is the highest of the studied glaciers, so this could also explain the mass gain in the first period (Figure 2a). But there is otherwise consistent thinning over the entire elevation range of both glaciers for all subsequent periods, with the greatest thinning rates for the most recent measurement period.

4. Discussion and Summary

[16] We demonstrate using a combination of maps, DEMS, and lidar profiles that the average rate of surface thinning on glaciers ranging in size from 5–1000 km^2 in western Svalbard has increased during the past decades. An increase in thinning rates implies that the rate of mass loss is increasing. While converting thinning rates directly to ice or water loss requires that there be no change in the spatial distribution of density over time, the close fit between the measured geodetic and elevation change inferred from ML mass balance (Figure 2a) suggests that density changes are negligible. Indeed, the magnitude and extent of density changes required to explain mean observed elevation changes on the study glaciers would be impossibly large.

[17] The three records have slightly different overall thinning signals (Figures 2a and 2b), which may reflect local climatic conditions, the different hypsometries of the glaciers, and different glacier flow dynamics. However, all of the investigated glaciers show thinning rates increasing with time. ML has the most up to date record, and shows that this acceleration in thinning continues right up to the present (2005).

[18] Increased glacier thinning is consistent with climate trends on Svalbard as recorded in the meteorological record from Longyearbyen (location shown in Figure 1), which begins in 1912. Summer temperatures have been rising since the 1960s [*Førland and Hanssen-Bauer*, 2003]; the trend for mean June–August (JJA) temperature is 0.04°C yr^{-1} for the 30-year period 1967–2006, and 0.17°C yr^{-1} for the 10-year period 1997–2006. The mean summer (JJA) temperature for the last five years (2001–2006) is nearly 6°C, the warmest five year period in the entire record, even warmer than the relatively mild 1930s, suggesting that the driver for Svalbard glacier changes is warmer summer temperatures causing additional melt. While winter precipitation (mostly snow) at Longyearbyen shows no clear long-term trend [*Førland and Hanssen-Bauer*, 2003], winter mass balance measurements at ML indicate a decreasing trend in winter accumulation since 1990 [*Hagen et al.*, 2003b].

[19] Thinning appears to increase most significantly on the upper parts of the studied glaciers (Figure 3). Changes in albedo will more strongly influence the response higher upglacier as surfaces there change from snow to bare ice. The trend toward less winter accumulation would result in relatively greater thinning rates from the lower albedo in the upper glacier, since the tongue more consistently has a low albedo during the summer.

[20] Recent GRACE measurements show significant mass loss over the broader area of Svalbard and NE Greenland, a greater mass loss than previously suspected and currently unexplained [*Chen et al.*, 2006]. Our results suggest that increased thinning on Svalbard could be partly responsible. The relatively large "footprint" of the GRACE data means that mass loss in NE Greenland cannot be considered alone, since mass loss Svalbard has the potential to influence results for the larger area. Surface deformation data from Ny-Ålesund, NW Svalbard as determined from GPS and VLBI data [*Sato et al.*, 2006] indicate a contemporary uplift rate which, if it were attributed solely to elastic uplift in response to mass loss from Svalbard glaciers,

would be equivalent to -0.75 m a^{-1}, in meters water equivalent. Again, this is a greater mass loss than prior estimates [*Dowdeswell et al.*, 1997; *Van de Wal and Wild*, 2001; *Hagen et al.*, 2003a, 2003b], which are based on assorted mass balance data averaged over variable periods, but roughly from the mid-1960s to 2000. The acceleration in thinning we observe implies a greater contribution from this region to sea level rise, even considering the concurrent reduction in glaciated area, which in western Svalbard amounts to only ~0.3% per year for the period 1936–1990 [*Nuth et al.*, 2007].

[21] **Acknowledgments.** Lidar data were collected by the UK NERC Airborne Research and Survey Facility and its analysis was funded through NERC grant NE/B505203/1 (SLICES). Norwegian Arctic Climate Impact Assessment (NorACIA) supported analysis of archived map and mass balance data. N.E.B. was funded through NERC studentship NER/S/A/2003/11279. GPS base stations for the lidar campaign were provided by the NERC Geophysical Equipment Facility. We thank Applied Imagery for supplying the Swansea group with QT Modeller and BAE Systems for their help and support with SOCET SET. Finally, we wish to thank Danny McCarroll, Matt King, Kim Holmén, for comments on an earlier draft, and Mark Dyurgerov and an anonymous reviewer for their helpful reviews, which greatly improved the paper.

References

Abdalati, W., W. Krabill, E. Frederick, S. Manizade, C. Martin, J. Sonntag, R. Swift, R. Thomas, J. Yungel, and R. Koerner (2004), Elevation changes of ice caps in the Canadian Arctic Archipelago, *J. Geophys. Res.*, *109*, F04007, doi:10.1029/2003JF000045.

ACIA (2005), *Arctic Climate Impact Assessment*, 1024 pp., Cambridge Univ. Press, New York.

Arendt, A. A., K. A. Echelmeyer, W. D. Harrison, C. S. Lingle, and V. B. Valentine (2002), Rapid wastage of Alaska glaciers and their contribution to rising sea level, *Science*, *297*, 382–386.

Bamber, J., W. Krabill, V. Raper, and J. Dowdeswell (2004), Anomalous recent growth of part of a large Arctic ice cap: Austfonna, Svalbard, *Geophys. Res. Lett.*, *31*, L12402, doi:10.1029/2004GL019667.

Bamber, J. L., W. Krabill, V. Raper, J. A. Dowdeswell, and J. Oerlemans (2005), Elevation changes measured on Svalbard glaciers and ice caps from airborne LIDAR data, *Ann. Glaciol.*, *42*, 202–208.

Chen, J. L., C. R. Wilson, and B. D. Tapley (2006), Satellite gravity measurements confirm accelerated melting of Greenland Ice Sheet, *Science*, *313*, doi:10.1126/science.1129007.

Church, J. A., J. M. Gregory, P. Huybrechts, M. Kuhn, K. Lambeck, M. T. Nhuan, D. Qin, and P. L. Woodworth (2001), Changes in sea-level, in *IPCC Third Scientific Assessment of Climate Change*, edited by J. T. Houghton et al., pp. 639–694, Cambridge Univ. Press, Cambridge.

Comiso, J. (2006), Arctic warming signals from satellite observations, *Weather*, *61*, 70–76.

Dowdeswell, J. A., et al. (1997), The mass balance of circum-Arctic glaciers and recent climate change, *Quat. Res.*, *48*, 1–14.

Etzelmüller, B., G. Vatne, R. S. Odegard, and J. L. Sollid (1993), Mass-balance and changes of surface slope, crevasse and flow pattern of Erikbreen, Northern Spitsbergen: An application of a geographical information system (GIS), *Polar Res.*, *12*, 131–146.

Førland, E. J., and I. Hanssen-Bauer (2003), Past and future climate variations in the Norwegian Arctic: overview and novel analyses, *Polar Res.*, *22*, 113–124.

Hagen, J. O., O. Liestøl, E. Roland, and T. Jørgensen (1993), Glacier atlas of Svalbard and Jan Mayen, *Norsk Polarinst. Meddelelser*, *129*, 160 pp.

Hagen, J. O., K. Melvold, J. F. Pinglot, and J. A. Dowdeswell (2003a), On the net mass balance of the glaciers and ice caps of Svalbard, Norwegian Arctic, *Arct. Antarct. Alp. Res.*, *35*, 264–270.

Hagen, J. O., J. Kohler, and K. Melvold (2003b), Glaciers in Svalbard: Mass balance, runoff, and freshwater flux, *Polar Res.*, *22*, 145–159.

James, T. D., T. Murray, N. E. Barrand, and S. L. Barr (2006), Extracting photogrammetric ground control from lidar DEMs for change detection, *Photogramm. Rec.*, *21*(116), 310–326.

Jiskoot, H., T. Murray, and P. J. Boyle (2000), Controls on the distribution of surge-type glaciers in Svalbard, *J. Glaciol.*, *46*(154), 412–422.

Kaser, G., J. G. Cogley, M. B. Dyurgerov, M. F. Meier, and A. Ohmura (2006), Mass balance of glaciers and ice caps: Consensus estimates for 1961–2004, *Geophys. Res. Lett.*, *33*, L19501, doi:10.1029/2006GL027511.

Krabill, W., et al. (2000), Greenland Ice Sheet: High-elevation balance and peripheral thinning, *Science*, *289*, 428–430.

Lindsay, R. W., and J. Zhang (2005), The thinning of Arctic sea-ice, 1988–2003: Have we passed a tipping point?, *J. Clim.*, *16*, 4879–4894.

Luckman, A., T. Murray, R. de Lange, and E. Hanna (2006), Rapid and synchronous ice-dynamic changes in East Greenland, *Geophys. Res. Lett.*, *33*, L03503, doi:10.1029/2005GL025428.

Nuth, C., J. Kohler, H. F. Aas, O. Brandt, and J. O. Hagen (2007), Glacier geometry and elevation changes on Svalbard (1936–90), *Ann. Glaciol.*, *46*, in press.

Paterson, W. S. B. (1994), *The Physics of Glaciers*, 481 pp., Pergamon, New York.

Pillewizer, W. (1962), German Spitsbergen expedition 1962, *Petermanns Geogr. Mitt.*, *106*, 286.

Rignot, E., and P. Kanagaratnam (2006), Changes in the velocity structure of the Greenland ice sheet, *Science*, *311*, 986–990.

Santer, B. D., et al. (2005), Amplification of surface temperature trends and variability in the tropical atmosphere, *Science*, *309*, 1551–1556.

Sato, T., J. J. Okuno, J. Hinderer, D. S. MacMillan, H.-P. Plag, O. Francis, R. Falk, and Y. Fukuda (2006), A geophysical interpretation of the secular displacement and gravity rates observed at Ny-Ålesund, Svalbard in the Arctic: Effects of post-glacial rebound and present-day ice melting, *Geophys. J. Int.*, *165*, 729–743.

Serreze, M. C., J. E. Walsh, F. S. Chapin, T. Osterkamp, M. Dyurgerov, V. Romanovsky, W. C. Oechel, J. Morison, T. Zhang, and R. G. Barry (2000), Observational evidence of recent change in the northern high-latitude environment, *Clim. Change*, *46*, 159–207.

Stroeve, J. C., M. C. Serreze, F. Fetterer, T. Arbetter, W. Meier, J. Maslanik, and K. Knowles (2005), Tracking the Arctic's shrinking ice cover: Another extreme September minimum in 2004, *Geophys. Res. Lett.*, *32*, L04501, doi:10.1029/2004GL021810.

Thomas, R., E. Frederick, W. Krabill, S. Manizade, and C. Martin (2006), Progressive increase in ice loss from Greenland, *Geophys. Res. Lett.*, *33*, L10503, doi:10.1029/2006GL026075.

Van de Wal, R. S. W., and M. Wild (2001), Modelling the response of glaciers to climate change by applying volume-area scaling in combination with a high resolution GCM, *Clim. Dyn.*, *18*, 359–366.

H. F. Aas, O. Brandt, J. Kohler, and C. Nuth, Norwegian Polar Institute, Polar Environmental Centre, N-9296 Tromsø, Norway.

N. E. Barrand, T. D. James, A. Luckman, and T. Murray, School of the Environment and Society, Swansea University, Swansea SA2 8PP, UK.